Enhanced performance photon-counting time-of-flight sensor

Ryan E. Warburton, Aongus McCarthy, Andrew M. Wallace, Sergio Hernandez-Marin, Sergio Cova*, Robert A. Lamb† and Gerald S. Buller

Heriot-Watt University, Riccarton, Edinburgh EH14 4AS, UK
G.S.Buller@hw.ac.uk
**Dipartmento di Elettronica e Informazione, Piazza Leonardo Da Vinci 32, 20133 Milano, Italy*
†QinetiQ, St. Andrews Road, Malvern, Worcestershire WR14 3PS, UK

Abstract: We describe improvements to a time-of-flight sensor utilising the time-correlated single-photon counting technique employing a commercially-available silicon-based photon-counting module. By making modifications to the single-photon detection circuitry and the data analysis techniques, we experimentally demonstrate improved resolution between multiple scattering surfaces with a minimum resolvable separation of 1.7 cm at ranges in excess of several hundred metres.

OCIS codes: (120.0120) Instrumentation, measurement and metrology; (040.6040) Silicon; (280.3640) Lidar; (040.3780) Low Light Level.

References and links

1. A.M. Wallace, G.S. Buller, A.C. Walker, J.S. Massa and M. Umasuthan, "As easy as TCSPC? Depth imaging and 3D metrology based on time-correlated single-photon counting," Image Process. Europe **2** 32-35 (1998).
2. A.M. Wallace, G.S. Buller, and A.C. Walker, "3D imaging and ranging by time-correlated single-photon counting," Computing & Control Engineering Journal **12**, 157-168, (2001).
3. J.S. Massa, A. M. Wallace, G.S. Buller, S.J. Fancey and A.C. Walker, "Laser depth measurement based on time-correlated single-photon counting," Opt. Lett. **22**, 543-545, (1997).
4. M. Umasuthan, A.M. Wallace, J.S. Massa, G.S. Buller, A.C. Walker, "Processing time-correlated single-photon counting data to acquire range images," IEE Proc. Vision, Image Signal Process. **145**, 237-243 (1998).
5. G.S. Buller, R.D. Harkins, A. McCarthy, P.A. Hiskett, G.R. MacKinnon, G.R. Smith, R. Sung and A.M. Wallace, "A multiple wavelength time-of-flight sensor based on TCSPC," Rev. of Sci. Instrum. **76**, 083112 (2005).
6. A.M. Wallace, R.C.W. Sung, G.S. Buller, R.D. Harkins, R.E. Warburton and R.A. Lamb, "Detecting and characterising return in a multi-spectral pulsed LaDAR system," IEE Proc. Vision Image Signal Process. **153**, 160-172 (2006).
7. I. Rech, I. LaBanca, M. Ghioni and S. Cova, "Modified single photon counting modules for optimal timing performance," Rev. Sci. Instrum. **77**,033104 (2006).
8. S. Richardson and P. Green, "On Bayesian analysis of mixtures with an unknown number of components," J. Roy. Statist. Soc. Ser. B, **59**, 731–792, (1997).
9. S. Pellegrini, G.S. Buller, J.M. Smith, A.M. Wallace, S. Cova, **"**Laser-based distance measurement using picosecond resolution time-correlated single-photon counting," Meas. Sci. Technol. **11**, 712-716 (2000).

1. Introduction

Previous work on using time-of-flight sensing utilizing time-correlated single-photon counting (TCSPC) techniques has been pursued for a number of years [1, 2, 3]. Initially, much of this work was used for 3-D reverse modelling of large objects under laboratory conditions. The technique allows for high resolution (10's μm depth resolution) when large numbers of single-photon returns are acquired from a stationary surface [4]. More recently, the technique has

#75858 - $15.00 USD Received 11 October 2006; revised 18 December 2006; accepted 20 December 2006

been used at longer distances (i.e. >1 km) for the analysis and identification of targets containing more than one scattering surface [5].

In this paper we describe the improved capabilities of the multiwavelength TCSPC-based sensor with the introduction of a modified detector. The optical system has been described in detail in [5] as have the some of the computational data processing techniques [6]. A brief review of the system and its components will be given along with the experimental procedure and results. The experimental analysis will concentrate on the resolving of separation between two surfaces at a range of more than 300 m.

2. System setup

Figure 1 represents a system schematic. For efficient collection of returns from the target, a 200 mm Meade catadioptric telescope was employed, as described more fully in [5]. Around its circumference, 6 pulsed diode-lasers were mounted at 60º intervals. The lasers' operating wavelengths are 630 nm, 686 nm, 780 nm, 841 nm, 911 nm and 975 nm. These wavelengths were chosen so as to be in the high efficiency region of the silicon single-photon avalanche diode (SPAD) detectors used and to avoid excessive atmospheric attenuation. For the specific set of results presented in this paper, only the 630 nm wavelength laser was used with a repetition rate of 20MHz and an average output power level of ~3 μW. The back-scattered light from the target was collected at the image plane of the telescope in an optical fibre. A diffraction grating housed in the optical routing module split the incoming light into the six constituent laser wavelengths; these were then focussed into fibres which connect to six independent SPADs, one detector corresponding to each of the wavelengths. The silicon SPAD used in this paper was a Perkin Elmer SPCM photon-counting module (SPCM-AQR-12-FC 5699 Rev F). The photon-counting card used (Becker & Hickl SPC-600) worked in reverse mode; where the timing process was started by the photon event and the stop signal was provided by a synchronized signal from the laser driver. A histogram of photon arrival times was recorded by the photon-counting module over a user-defined period of time.

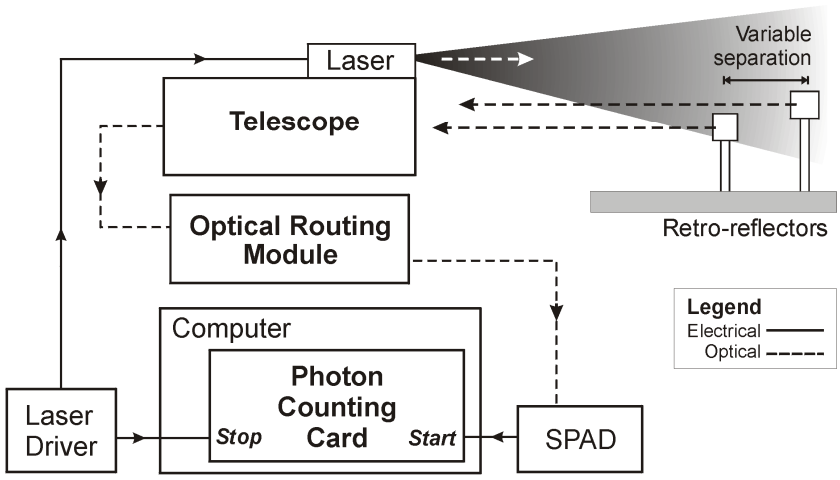

Fig. 1. System Schematic. The target consisted of two retro-reflectors with variable separation.

3. Experiment motivation and procedure

The timing jitter of the detectors used plays a major role in determining the system resolution. The timing jitter is usually described by the full width at half maximum (FWHM) of the system response to a short optical input signal. As the timing jitter increases, the temporal return peak representing a surface will widen, and consequently there will be a greater difficulty in resolving neighbouring reflective surfaces. In this system, the dominant

#75858 - $15.00 USD Received 11 October 2006; revised 18 December 2006; accepted 20 December 2006

contribution to jitter was from the single-photon detector, and since we are attempting to resolve the separation of two target returns, it is beneficial to use a detector with low jitter. In this work we used commercially-available silicon SPADs to detect the returns from the target. These detectors, referred to as "Unmodified SPAD," had a timing jitter of approximately 600 ps at low count rates as shown in Fig. 2(a). Due to high ambient background levels of light found in daylight operation in this application, we normally operate in the high count rate regime, at approximately 1 Mega-count per second where the jitter increases to 800 ps FWHM, thus decreasing the overall depth resolution of the system. Recently, one of these modules was modified by the group at Politecnico di Milano by improving its output circuitry, as described in [7]. In this paper this detector will be referred to as "Modified SPAD". Referring back to Fig. 2(a), with the modified SPAD a jitter of less than 400 ps was attainable, and importantly, the jitter is far less dependent on the count rate. Figure 2(b) represents a study of the timing position of the peak of the instrumental response within the photon-counting histogram versus count rate. Here we observe that as the count rate increases, there is a clear shift of the maximum of the temporal peak when using the unmodified SPAD. This would have an adverse effect on the system capabilities especially in the case of fluctuating signal returns, as is found with the photon return signal in a turbulent environment. With the modified SPAD, there is only a relatively slight deviation in the peak position with changing count rate.

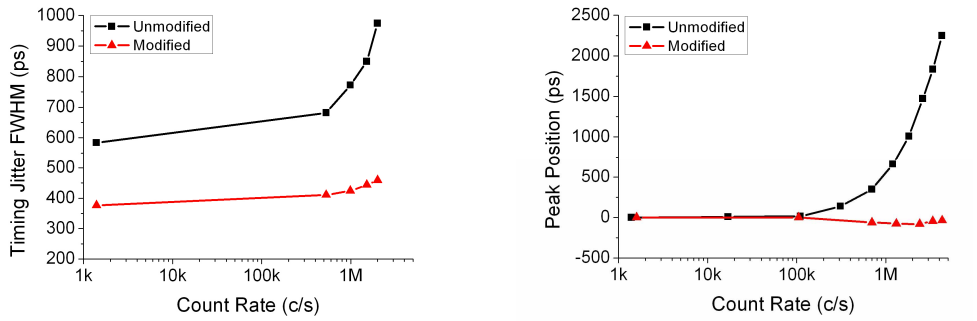

Fig. 2. (a) SPAD timing jitter and (b) peak position as a function of count rate for both SPADs.

A bench-test for our ranging system is its ability to distinguish two surfaces separated by a finite distance. To simulate two reflecting surfaces, two retro-reflecting corner-cubes were placed in kinematic mounts on an optical rail at a distance of 330 m from the transceiver equipment as shown in Fig. 1. We were therefore able to vary the distance between these surfaces, from a maximum of 70 cm to a minimum of 1.7 cm.

At each separation a histogram was recorded for analysis using two different integration, or collection, times of 1 s and 30 s. All experiments were conducted under identical ambient light conditions.

When the corner-cubes are separated by a resolvable distance, two separate defined peaks can be seen in the recorded histogram as shown in Fig. 3.

#75858 - $15.00 USD Received 11 October 2006; revised 18 December 2006; accepted 20 December 2006

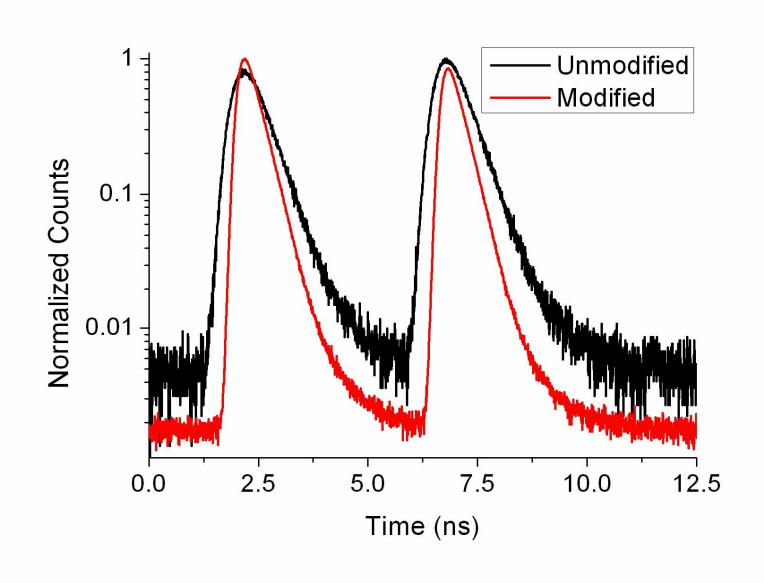

Fig. 3. Histogram of normalized returns from two corner-cubes separated by 70cm, recorded using both SPAD detectors, with photon counts normalized to the same height for illustrative purposes. In this case, the histogram is shown on a semi-logarithimic plot.

As the separation of the surfaces decreases, the peaks representing the position of the surfaces begin to merge and, consequently, it becomes increasingly difficult to calculate their separation. If we use a SPAD with a faster response time, the minimum resolvable separation will decrease since the peaks will not merge at reduced target surface separations as in the case of a slower detector, as illustrated in Fig. 4.

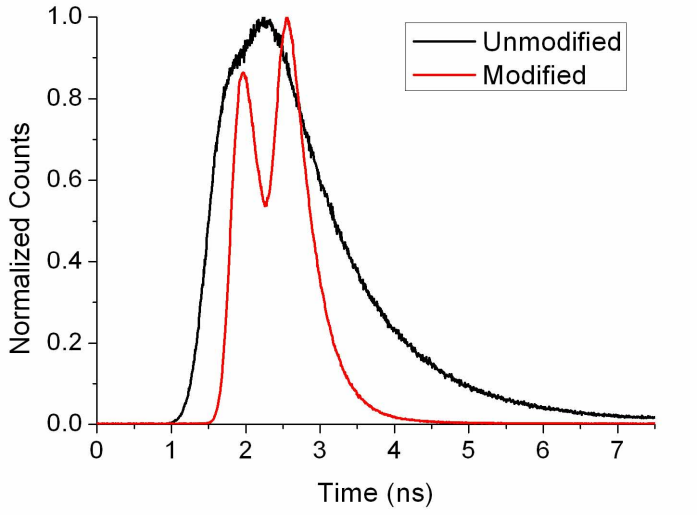

Fig. 4. Histogram of returns from two corner-cubes separated by 9.2 cm, recorded using both SPADs, with photon counts normalized to the same maximum height for illustrative purposes.

#75858 - $15.00 USD Received 11 October 2006; revised 18 December 2006; accepted 20 December 2006

A number of different methods to calculate peak separations have been used [5, 6]. The centroid method was used to find the average central position of these peaks and then the difference between these temporal, and hence spatial, positions. This method gives a preliminary indication of resolution, although more sophisticated models are presented below. At reduced separations, the centroid method is likely to fail when two distinct peaks are not clearly distinguishable.

4. Experimental results

In terms of signal-to-background considerations, we follow the elementary descriptions provided previously in [9]. The upper limit of signal-to-background will be determined by photon statistics and is simply the square root of the maximum signal, n_{sig}. However the effect of the background level counts (denoted by a mean level n_B) caused by both ambient light and detector dark-counts reduce the signal-to-background in the following manner:

$$SBR = \frac{n_{sig}}{(n_{sig} + n_B)^{\frac{1}{2}}} \tag{1}$$

Comparing the SBR for both SPADs for the same collection time under identical experimental conditions using a single target surface, the modified SPAD presents approximately double the SBR of that of the unmodified SPAD. This is caused by the reduction in jitter found in the case of the modified SPAD which, when coupled with no change in the detector efficiency, will result in a greater peak height than the unmodified SPAD used under the same experimental conditions. Evidence of this can be seen in Figure 3, where both peak heights are normalized, but which results in a reduction in background level for the unmodified SPAD.

For a full comparison of the two SPADs we can compare the actual separation to the calculated separation. Measurements were taken at 19 different separations; from 71.2 cm to 1.7 cm using both SPADs as shown in Fig. 5.

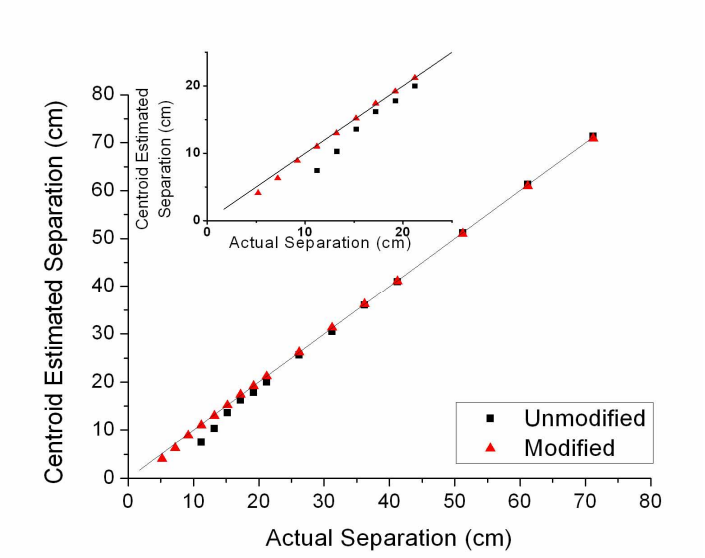

Fig. 5. Calculated separation using centroid method vs. actual separation for both SPADs, the black line shows the case of perfect agreement. The insert shows an expansion of the graph at the lower surface separations.

#75858 - $15.00 USD Received 11 October 2006; revised 18 December 2006; accepted 20 December 2006

At larger separations, both SPAD detectors perform well and the calculated separation agrees with the actual separation. As the corner-cube separation is reduced, the peaks will merge into each other and make the resolving of individual surfaces more difficult. The higher jitter level of the unmodified SPAD will mean that this will be more obvious at smaller surface separations. As can be seen in Fig. 5, with the unmodified SPAD it becomes progressively more difficult to accurately resolve the surface separation at separations below ~20 cm and impossible to calculate at surface separations of less than 11.2 cm. However, with the modified SPAD, the agreement with the expected behaviour was very good at surface separations of down to 10 cm, and surface separations of down to 5.2 cm could be calculated with reasonable accuracy. For separations of less than 5 cm a different analysis approach was adopted, an example of which will be discussed later. This distance of 5 cm is commensurate with the improved timing jitter of ~400 ps with the modified SPAD. In terms of repeatability of results, we have performed multiple measurements on the same surface separation under the experimental conditions described above, and analysed the data. Over multiple measurements, we found that the repeatability of the range was within 0.5 mm.

To improve on the standard correlation method to detect the position and amplitude of peaks, especially when the signal to background level is very low, we have developed an improved method of data analysis by non-parametric bump-hunting and maximum likelihood estimation using Poisson statistics [6]. However, even that approach will fail if the signal levels are well below the background so we have further developed new algorithms based on Markov chain Monte Carlo (MCMC), and reversible jump MCMC techniques (RJMCMC) [8] to assess the number, positions and amplitudes of the returned signals from target surfaces. The combination of these two methodologies allows moves between models with different dimensionality (i.e. when the number of returns is not known) and within-model moves when the dimension is fixed. The main advantages of the underlying Bayesian approach of these techniques is that it provides a natural method for updating beliefs in response to new information and incorporates prior knowledge into the analysis. Furthermore, the MCMC methods provide an approximation of the full joint posterior distribution of the model parameters and therefore naturally represent the uncertainties inherent in any inferences from the data.

The complexity of these methods can be greatly reduced if we have a-priori information about the signal context. In these experiments the most important a-priori data that we can include are the instrumental response of the detector, and the number of anticipated peaks. Indeed, if we know that there are two peaks then the simple MCMC methodology can be employed. Although the algorithms are not yet fully optimised for the different SPAD response features, Fig. 6 shows the capabilities of such methods. The program is able to identify two peaks even when they are completely overlapped. Furthermore, Fig. 6 represents the computational results from data collected in an acquisition time of just 1 s. It should be noted that, currently, the algorithms used require several thousand iterations to find peaks within a histogram and hence the process is time-consuming. From Fig. 6, it is clear that this approach can reduce the surface separation resolution to at least ~1.7 cm in the case of the modified SPAD. For illustrative purposes, in Fig. 7 we show the photon return histogram for two corner-cubes for the minimum resolved separation of 1.7 cm, normalized to the same photon return maximum of a standard instrumental response as found from a single corner-cube return.

#75858 - $15.00 USD Received 11 October 2006; revised 18 December 2006; accepted 20 December 2006

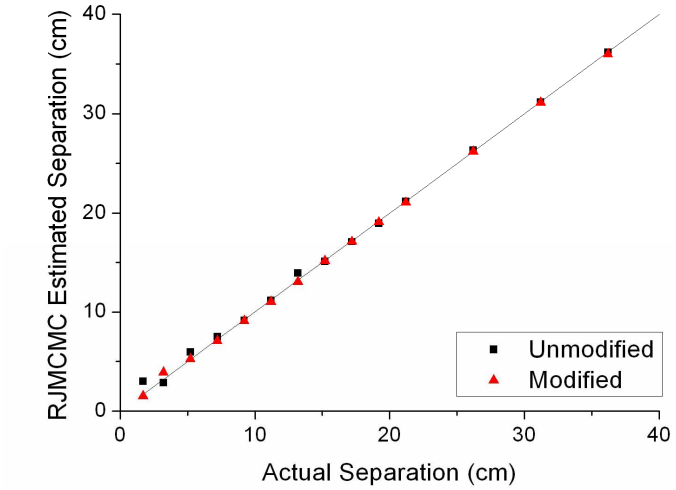

Fig. 6. Calculated separation using RJMCMC algorithm on data acquired in 1 sec vs. actual separation

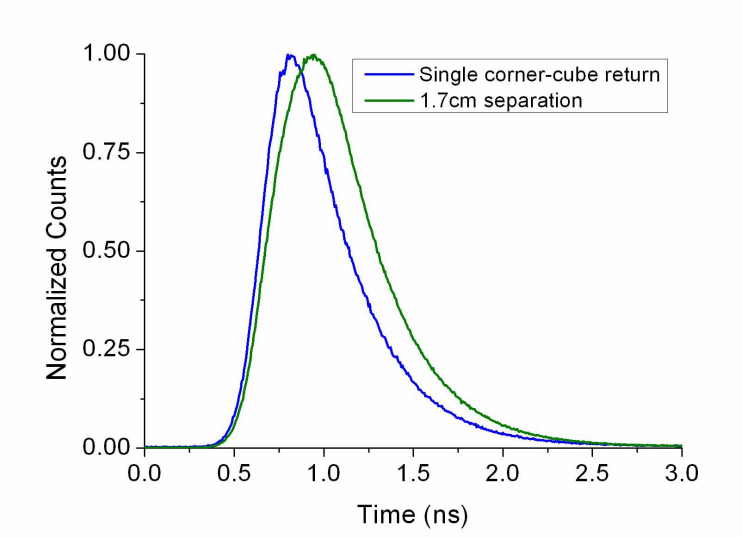

Fig. 7. Comparison of single corner-cube return and returns from corner-cubes separated by 1.7 cm.

5. Conclusions and further work

We have successfully demonstrated the increased depth resolution of the system using a detector with a lower timing jitter. Even with a simple centroid separation approach, we were able to distinguish between two surfaces separated by 5.2 cm at a distance of 330 m. Using the reversible jump Markov chain Monte-Carlo approach, the surface separation resolution can be as low as 1.7 cm. Whilst such resolution will have some dependence on signal to background ratio, it is likely that centimetre resolution distinguishing target surfaces can be achieved by this sensor at ranges of several kilometres under normal daylight operation.

In the future, it is hoped that new SPADs with even lower timing jitter will be employed, along with the development of real-time result-processing. It is also our intention to adapt the transceiver for scanning to increase the scope of the system's capabilities.

#75858 - $15.00 USD Received 11 October 2006; revised 18 December 2006; accepted 20 December 2006